frontiers | Frontiers in Energy Research

TYPE Original Research
PUBLISHED 10 March 2023
DOI 10.3389/fenrg.2023.1067623

Check for updates

OPEN ACCESS

EDITED BY
Young-Deuk Kim,
Hanyang Universiy, Republic of Korea

REVIEWED BY
Woo-Jin Jeon,
Korea Research Institute of Ships and Ocean Engineering, Republic of Korea
Ik-Tae Im,
Jeonbuk National University, Republic of Korea

*CORRESPONDENCE
Muhammad Burhan,
muhammad.burhan@kaust.edu.sa
Seung Jin Oh,
ohs8680@kitech.re.kr

SPECIALTY SECTION
This article was submitted to Process and Energy Systems Engineering, a section of the journal Frontiers in Energy Research

RECEIVED 13 October 2022
ACCEPTED 27 February 2023
PUBLISHED 10 March 2023

CITATION
Shoaib A, Burhan M, Chen Q and Oh SJ (2023), An artificial neural network-based performance model of triple-junction InGaP/InGaAs/Ge cells for the production estimation of concentrated photovoltaic systems.
Front. Energy Res. 11:1067623.
doi: 10.3389/fenrg.2023.1067623

COPYRIGHT
© 2023 Shoaib, Burhan, Chen and Oh. This is an open-access article distributed under the terms of the Creative Commons Attribution License (CC BY). The use, distribution or reproduction in other forums is permitted, provided the original author(s) and the copyright owner(s) are credited and that the original publication in this journal is cited, in accordance with accepted academic practice. No use, distribution or reproduction is permitted which does not comply with these terms.

An artificial neural network-based performance model of triple-junction InGaP/InGaAs/Ge cells for the production estimation of concentrated photovoltaic systems

Aisha Shoaib[1], Muhammad Burhan[2]*, Qian Chen[3] and Seung Jin Oh[4]*

[1]Department of Mechatronics and Control Engineering, University of Engineering and Technology, Lahore, Pakistan, [2]Water Desalination and Reuse Center, King Abdullah University of Science and Technology, Thuwal, Saudi Arabia, [3]Shenzhen International Graduate School, Institute for Ocean Engineering, Tsinghua University, Shenzhen, China, [4]Sustainable Technology and Wellness R&D Group, Jeju Division, Korea Institute of Industrial Technology (KITECH), Cheonan-Si, Republic of Korea

Analytical and empirical models analyze complex and non-linear interactions between the input–output parameters of the system. This is very important in the case of photovoltaic systems to understand their real performance potential. On the other hand, manufacturers of photovoltaic panels rate the maximum performance of the system under fixed lab conditions as per standard testing conditions (STCs) or nominal operating cell temperature (NOCT) standards of IEC. These ratings do not provide the actual production potential of the system in a field with fluctuating conditions of irradiance and temperature. For the case of a concentrated photovoltaic (CPV) system, utilizing multi-junction solar cells (MJCs), there is no commercial tool available to analyze the performance and production, despite some recent empirical models that also require post-processing of experimental data to be used in conventional models. In this study, an artificial neural network (ANN)-based performance model is presented for a multi-junction solar cell, which is not only convenient to apply but can also be easily expanded to predict the real-field performance of the CPV system of any designed size. In addition, the ANN-based model showed a high accuracy of 99.9% in predicting the performance output of MJCs as compared to diode-based empirical models available in the literature. The irradiance concentration at the cell area and the cell temperature are taken as inputs for the neural network. If both of these parameters are known, then the cell efficiency as an output can accurately predict the CPV performance for a field operation.

KEYWORDS

multi-junction solar cell (MJC), concentrated photovoltaic (CPV), photovoltaic (PV), artificial neural network (ANN), solar concentrator

1 Introduction

Energy is very important for the development of the modern world. However, sustainable energy is even more important for the survival of our environment (Bailek et al., 2018; Cho et al., 2019; Chen et al., 2020). Global emissions have increased by more than 20% since the last decade (Shahzad et al., 2017). Many renewable energy resources can be utilized to achieve the sustainability goal (Burhan et al., 2016a; Burhan et al., 2017a; Peng et al., 2020). Solar energy is the only capable renewable energy resource that can meet the current global energy needs (Burhan et al., 2018a; Hakimi et al., 2020). The solar photovoltaic system is the simplest technology to produce sustainable electricity. The most efficient photovoltaic system is the concentrated photovoltaic (CPV) system, using multi-junction solar cells (MJCs), as they offer the highest energy efficiency of 47.1% (NREL, 2022). However, the multi-junction solar cell has a more complex principle of operation compared to conventional single-junction solar cells (Oh et al., 2015; Burhan et al., 2016b; Muhammad et al., 2016). To lower the system cost, MJCs are operated under high irradiance concentrations (assets, 2020), and as a result, under high temperatures (Burhan et al., 2019a), low-cost solar concentrators replace the expensive solar cell material (Cherucheril et al., 2011; Burhan et al., 2019b). The response and the resultant I–V curve of the solar cell change immediately with even minor changes in temperature or irradiance concentration (Burhan et al., 2017b; Burhan et al., 2018b).

The manufacturers of photovoltaic panels rate their performance at certain conditions of radiation and temperature which are not achievable most of the time in real-field operations. Standard testing conditions (STCs) (IEC 60904-3) or nominal operating cell temperature (NOCT) (IEC 61215 and IEC 61646) are two IEC standards that are used to rate the performance of photovoltaic panels as per the defined laboratory conditions, AM 1.5 spectrum, 1,000 W/m^2 irradiance, and 25°C cell temperature (Burhan et al., 2017c). To analyze the real-field potential of the photovoltaic system, it is very important to understand and analyze its behavior with changing conditions. By only knowing the standard efficiency of PV panels, one cannot predict the actual energy production from photovoltaic panels under realistic changing weather conditions. There are well-developed empirical and analytical expressions for the performance analysis of conventional single-junction photovoltaic cells under sunlight. However, there are limited studies related to performance models of concentrated photovoltaic systems, which are only empirical relations (Burhan et al., 2018c; Burhan et al., 2021). In addition, the structure and operation of concentrated photovoltaic systems make the performance modeling of the CPV system complex due to many factors affecting its performance (Burhan et al., 2018d). The two main parameters dictating the output of the MJC-based CPV system are the irradiance concentration and cell temperature, assuming accurate solar tracking and maximum power point tracking during the operation. These are the two operational parameters varying throughout the operation as the rest of the system parameters related to optics and cell materials remain unchanged. A small change in the irradiance concentration generates a new set of temperature gradients of the MJC (Burhan et al., 2016c; Burhan et al., 2018e).

Due to multi-parameter dependency, the relationship between the input parameters of MJCs, such as concentration and temperature, and the output parameters such as efficiency, current, voltage, power, and temperature gradient is not linear. The irradiance concentration at the MJC area largely affects their temperature characteristics and electrical outputs (Theristis et al., 2016). The analytical expression is not able to easily define the performance characteristics of MJCs with such multi-parameter dependency. On the other hand, empirical expressions require some post-processing of input parameters to define the performance characteristics of the MJC-based CPV system. The artificial neural network (ANN) is an alternative approach to complex expressions and finds the link between input and output parameters in such non-linear cases of photovoltaic systems (Kalogirou, 2000). A set of hidden neurons and their corresponding layers are arranged such that their values and structures define the complex interaction between input and output parameters (Ghritlahre et al., 2020; Zeynali et al., 2020). This ANN approach provides a simple solution for such a complex task. However, extensive effort is needed to get a set of experimental data with a broad range of input parameters as the ANN is trained on such a set of experimental data (Burhan et al., 2019c; Motahar and Bagheri-Esfeh, 2020). An ANN is a very promising tool for complex and multivariable problems in the field of photovoltaics. It can be applied for the prediction and estimation of solar irradiance (Mellit et al., 2005a; Mellit et al., 2006), system capacity for both standalone and grid-connected applications (Mellit et al., 2005b; Mellit et al., 2007), electrical characteristics of the solar cell including I–V curves (Almonacid et al., 2010), and the overall production of the field installed system (Almonacid et al., 2011).

Due to the complexities of the MJC's electrical and thermal characteristics and structure of the CPV module, the ANN has the advantage over conventional performance models that require an understanding and simulations of the complex physical phenomena involved in the CPV performance. In addition, they do not require detailed information on the material and manufacturing of the system. Also, there is no need for specific modeling software (Almonacid et al., 2017). There are many commercial tools available to simulate the performance of conventional photovoltaic systems, i.e., HOMER (HOMER, 2015), RAPSIM, TRNSYS + HYDROGEMS, ARES, SOMES, HYBRIDS2, SOLSIM, INSEL (Bernal-Agustin and Dufo-Lopez, 2009), and iHOGA (iHOGA, 2004). However, none of these tools can handle MJC-based CPV systems. Therefore, in our previous study (Burhan et al., 2017b), an empirical correlation was proposed for the performance prediction of the MJC-based CPV system. However, it requires complex processing of experimental data to determine the temperature gradients of open-circuit voltage and short-circuit current, although carrying out such an approach is not simple. Although the CPV system can only respond to the direct normal irradiance of solar energy, it is also a difficult parameter to predict and analyze. However, there are many studies on ANNs to predict the normal irradiance for concentrated photovoltaic (CPV) applications. In this paper, the focus is on the development of a performance model of the MJC-based CPV system using an artificial neural network, equivalent to an empirical model (Burhan et al., 2017b), with a higher accuracy and a simple set of input–output parameters. The ANN is developed for triple-junction InGaP/InGaAs/Ge MJCs, which was successfully able to provide cell efficiency up to a concentration factor of ×550 and a temperature

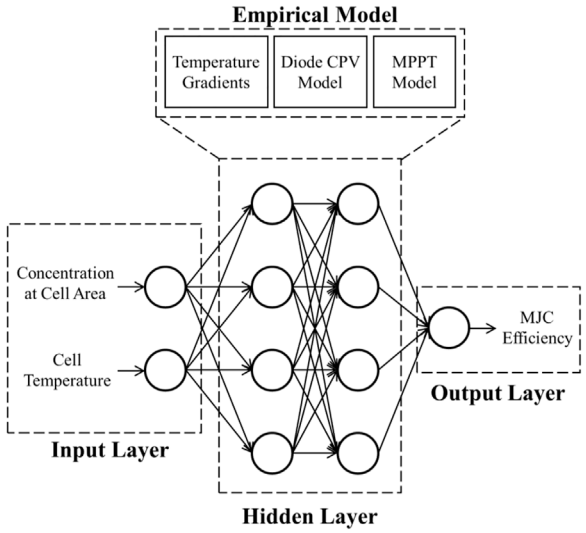

FIGURE 1
Graphical representation of the ANN and its comparison with the empirical CPV model.

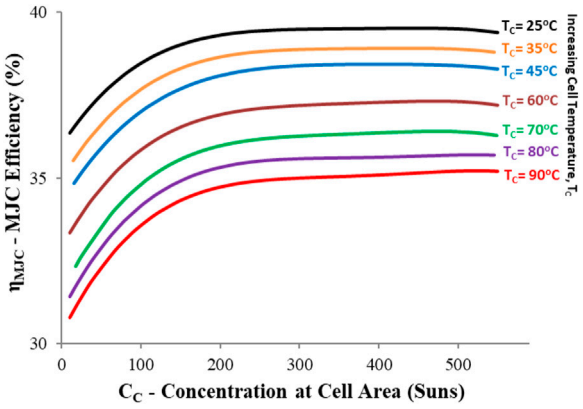

FIGURE 2
Experimental data for the MJC at different irradiance concentrations and cell temperatures.

range of 25–90°C. A detailed comparison of the proposed ANN configuration with our previously presented model is provided showing a great improvement in the accuracy with very less required information and computational effort/programming.

In this paper, the materials and methodology are discussed first, in which, first, the comparison of the ANN with empirical models is presented. Second, there is a detailed discussion on the collection of experimental data for the training and testing of the ANN. Lastly, the methodology is presented, in which the use of MJC data obtained from a trained ANN is discussed to calculate the performance of the CPV module. The constant parameters and algorithm used to train the ANN are also discussed in Section 2. In Section 3, the training accuracy of the ANN is presented first with mean squared error (MSE) and regression plots. The MJC performance data obtained from the trained ANN are compared against empirical models and experimental data. Lastly, the MJC performance data from the trained ANN are used to predict the real-field power output of the CPV system against the actual available weather data.

2 Materials and methods

2.1 Artificial neural network and the empirical model

Figure 1 shows the graphical representation of a typical artificial neural network. The ANN consists of three kinds of layers and their associated neurons. The first layer represents the input layer, and the number of neurons in input layers is equal to the number of input parameters. In the current study, the irradiance concentration at the cell area and the cell temperature are the two inputs for the neural network, as these two parameters are important to determine the performance of the MJC. The last layer represents the output layer, and similarly, the number of neurons in the output layer represents the number of output parameters. In this study, the cell efficiency is taken as the output parameter, as it not only gives the first performance impression of the multi-junction solar cell but all other parameters can also be calculated if the cell efficiency is known. Even the energy output of the CPV system can be calculated if the input power and receiver area are known. A detailed discussion of the calculation of the associated MJC parameters will be given at the end of this section. Other layers in between input and output layers are called hidden layers. The number of hidden layers, the number of associated neurons in these hidden layers, and the associated values of these neurons represent the complex interaction between input and output parameters. The structure of these trained hidden layers replaces the need for a conventional empirical model. The graphical representation of the ANN and its comparison with the empirical CPV model are given in Figure 1.

2.2 Experimental setup and data preparation for the ANN

To get the structure and associated values of the hidden layers, the ANN is trained for a broad set of data of input and output parameters. Figure 2 shows the experimental data for the MJC solar efficiency against the concentration of solar radiations at the cell area, for different values of cell temperature. The detailed values of the training dataset for input and output parameters are given in Table A1. To ensure accuracy, a large set of training data containing 315 sample values are considered. It is very important to note that the data presented in this study are based on the performance of the MJC, not the CPV system. To generalize the dataset, any design parameter such as the area of the MJC and concentrator area is not considered. Hence, the ANN model is trained for the performance of the MJC, and once the MJC performance parameters are known, the CPV power output can be determined with the required design parameters.

Figure 3 shows the schematic of the experimental setup typically utilized to record the performance characteristics of

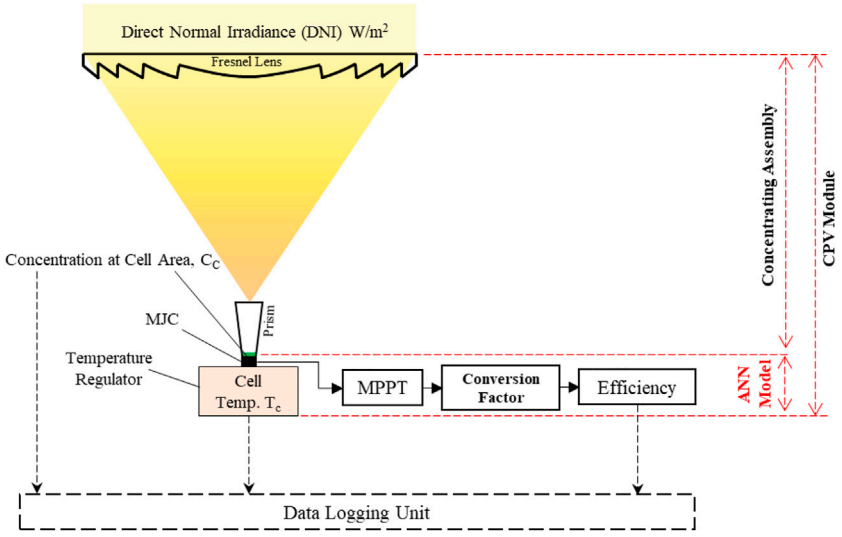

FIGURE 3
Schematic of the experimental setup to record the MJC performance.

the MJC. It is important to mention here that the triple-junction InGaP/InGaAs/Ge MJC was provided by Arima company and so were its performance data. The portion of the experimental setup considered in the training of the ANN consists of an MJC, a temperature regulator to set the cell temperature value, maximum power point tracking (MPPT) to maximize the output, and the conversion/constant parameters to determine the cell efficiency. The red dotted lines in Figure 3 represent the domain of the ANN model, concentrating assembly, and CPV module. The black dotted lines represent the flow of the recorded data to the data logger, and the solid black lines are used to label the different components in the system. The concentration value considered is the amount of radiation concentrated directly over the cell area. This irradiance concentration value is different than the irradiance value that is normally considered in conventional PV models. The irradiance represents the amount of solar radiation received per unit area by the solar concentrator. However, the concentration value considered in the training dataset represents the amount of concentrated radiation collected over a unit area of the MJC. The temperature regulator ensures a set value of cell temperature. The electrical output of the MJC is passed through the MPPT module, which ensures that the MJC is operating at this maximum efficiency point of the I–V curve. The output of the MJC is then stored in the data logging unit, in the form of cell efficiency after applying the associated conversion factors and design parameters of the experimental setup. The values of irradiance concentration and cell temperature are also recorded simultaneously. The conversion factor shown in Figure 3, to convert the power output of the MJC into efficiency, is given by

$$\eta_{MJC} = \frac{P_{MJC}}{P_{input}} = \frac{I_{mppt} \times V_{mppt}}{C_C \times A_C \times 1000}, \quad (1)$$

where "I_{mppt} and V_{mppt}" define the current and voltage output of the MJC after the MPPT module, respectively. The term A_c represents

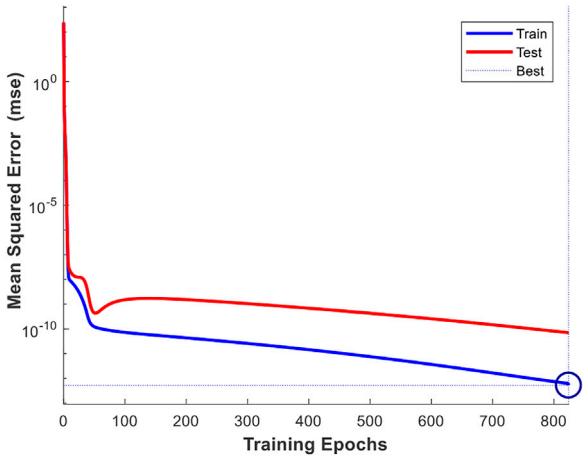

FIGURE 4
Mean squared error plot during the training and testing phase of the ANN of MJCs.

the cell area. However, the constant value "1,000" in the denominator of Eq. 1 is used to convert concentration units from suns to W/m^2.

2.3 ANN to CPV performance prediction

With the proposed ANN model, although it is trained for the performance of a single MJC, the power output of the CPV module can be easily determined. To estimate the output of the CPV module, it is important to determine the size and characteristics of the concentrating assembly. If the optical efficiency of CPV concentrating is represented by "η_{op}," then the power output of the CPV module, "P_{CPV}," is given by

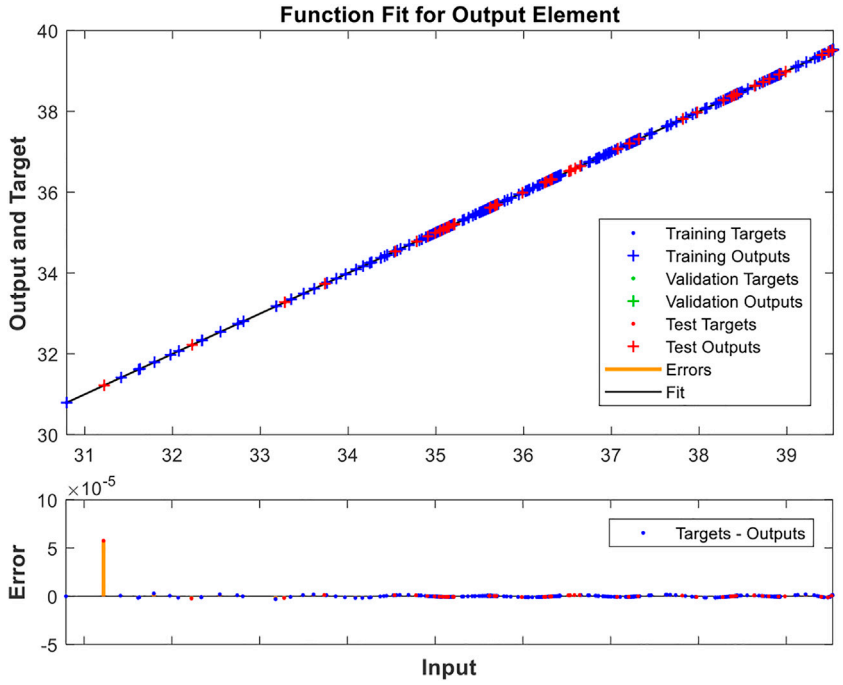

FIGURE 5
Function-fit plot for the trained ANN of MJCs.

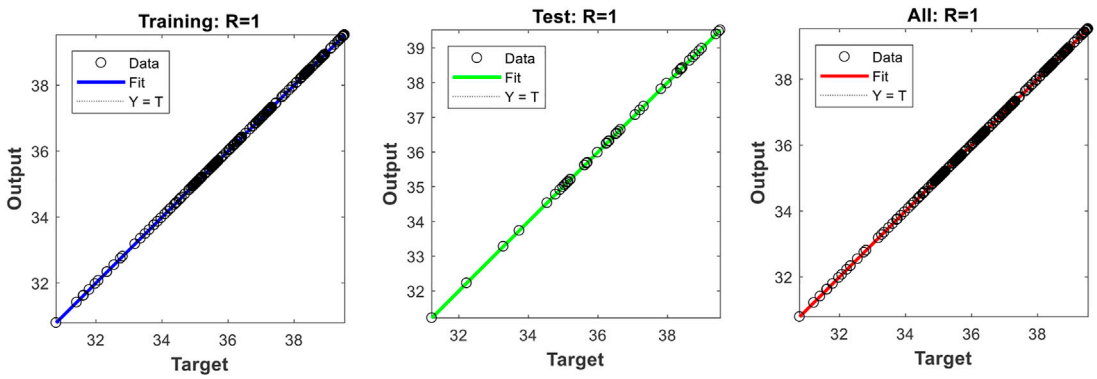

FIGURE 6
Regression plot for the trained ANN of MJCs.

$$P_{CPV} = N_C \times \left(\eta_{MJC} \times \eta_{op} \times DNI \times A_{lens}\right), \quad (2)$$

where "η_{MJC}" represents the MJC efficiency and 'A_{lens}' represents the effective area of the solar concentrator. The terms in the bracket represent the power output of a single MJC, and when it is multiplied by the total number of MJCs in the module, i.e., "N_C," then the total power output of the CPV module can also be determined. However, the optical efficiency of the CPV concentrating assembly is based on the material and number of optical elements. For a PMMA Fresnel lens-based assembly, its typical value is around 75%, and for a reflector-based Cassegrain assembly, it can range from 85% to 90%. It is also important to mention here that the CPV efficiency is the product of the MJC and concentrating assembly efficiencies, i.e.,

$$\eta_{CPV} = \eta_{MJC} \times \eta_{op}. \quad (3)$$

2.4 ANN training, validation, and testing

The collected experimental dataset was then used in the Neural Network Toolbox (nftool) of MATLAB. The input dataset (cell temperature, T_C, and the concentration at the cell area, C_C) is a matrix of 2 × 315, and the output dataset (cell efficiency, η_{MJC}) is a

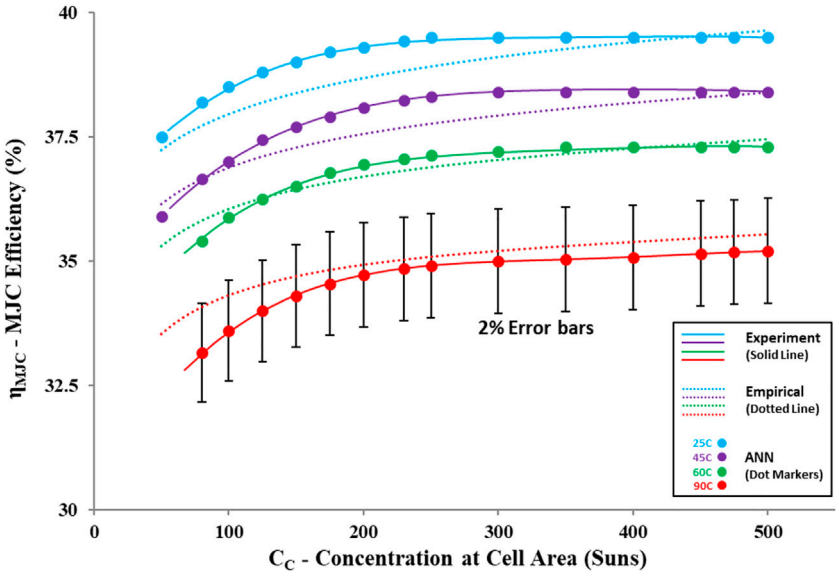

FIGURE 7
Comparison of the ANN-based MJC performance with the experimental data and empirical model values.

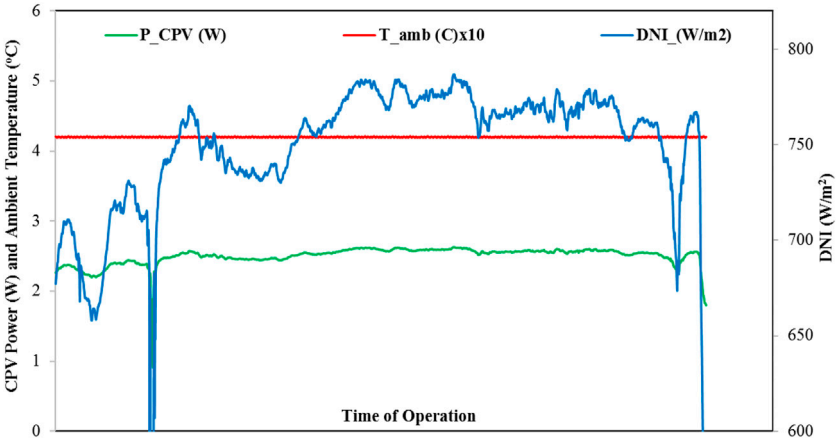

FIGURE 8
ANN-based predicted power output of the CPV system with weather data of the DNI and ambient temperature.

1 × 315 matrix. For training purposes, only 70% of the data points (221) were reserved, while the remaining data points were dedicated for validation and testing purposes, i.e., 15% (47 each). The validation and testing data points were selected randomly from whole datasets, and the remaining points were selected as the input for the training of the ANN. In this work, there is only one hidden layer comprising 10 hidden neurons. For the training algorithm, Bayesian regularization was used for better accuracy, as it provides the best relevance of input parameters to the neural network training, known as the ARD method (Lampinen and Vehtari, 2001). However, while using the scaled conjugate gradient and Levenberg–Marquardt, the regression accuracy dropped significantly.

3 Results and discussion

By using the Bayesian regularization algorithm, the ANN was trained with the backpropagation technique to minimize the mean squared error of targeted and output values. The training was initially started for 1,000 epochs. However, the algorithm converged at 824 epochs, where the MSE was the lowest, as

shown in Figure 4. The plot for the mean squared error of target and output values during the training and testing phase of the ANN is shown in Figure 4. On the other hand, the plot fit for target and output values against input data is shown in Figure 5. It can be seen that the error value is almost zero throughout the input range. This can also be verified by regression plots of the training and testing phases of the ANN as the regression value appears as 1 for both the cases, Figure 6. This shows that the current methodology is perfectly used to train and test the ANN for the performance prediction of MJCs. Due to the high accuracy, the algorithm did not need to validate the ANN. It is important to mention here that such a high accuracy was obtained using the Bayesian regularization algorithm. However, while using the scaled conjugate gradient and Levenberg–Marquardt, the regression accuracy dropped significantly ($R < 1$).

To verify the accuracy of the trained ANN, a comparison of the output data of the ANN is compared against the experimental data and the data obtained from the conventional empirical model, as shown in Figure 7. First of all, it can be seen that although the empirical model (Burhan et al., 2017b) is trying to follow the efficiency trend of the experimental data, there is still a significant contradiction between actual and calculated values. Although the empirical model is within the 2% error range of the experimental data, the efficiency points obtained through the trained ANN are showing a perfect agreement with the experimental data at various conditions of the concentration and temperature. The ANN prediction is 99.9%, matching the targeted experimental value, as depicted by the regression coefficient "R" in Figure 6. This shows that the ANN is not only simplifying the conventional approach of empirical models but the accuracy of the predicted data is also increased significantly, even when compared with ANN–CPV-based models available in the literature with 2.91% (Rivera et al., 2013) and 3.3% (Almonacid et al., 2013) error ranges, respectively. This will not only simplify the problems but also reduce the computational time. One of the key points of the high accuracy of the ANN is identifying and selecting the key input parameters, which are directly impacting the system performance.

To utilize the trained ANN in the real-field performance prediction of the CPV system performance, the power output of the CPV module consisting a single MJC is presented in Figure 8, against the actual direct normal irradiance (DNI) profile, measured using a pyrheliometer mounted on a two-axis solar tracker, along with the ambient temperature. It is important to mention here that the CPV power output shown here is based on the performance of MJCs obtained through the trained ANN. The DNI is defining the irradiance concentration at the area of MJCs with a concentrator area of 12 cm × 12 cm and an optical efficiency of 75%. On the other hand, the ambient temperature is defining the cell temperature, which is approximated at 40°C higher than the ambient temperature (Burhan et al., 2016d). This shows that with the proposed trained ANN of MJCs, one can easily predict the real production potential of the CPV system if the solar potential and weather conditions are known, which are mostly available through data centers of weather stations. Therefore, instead of relying on the maximum rated performance of the photovoltaic system, the real energy/power output of the CPV system can be easily predicted with ANN-based techniques, with a need for complex non-linear expressions and correlations.

4 Conclusion

An artificial neural network-based performance model is successfully trained and tested for the performance prediction of the multi-junction solar cell. In comparison to the conventional empirical model, with a 2% error range, the ANN-based model showed a high level of 99.9% accuracy in the solar cell efficiency prediction by knowing the cell temperature and the concentration at the cell area. The use of the Bayesian regularization algorithm for the ANN training increased the regression factor R from 0.97 to 1, as compared to conjugate gradient and Levenberg–Marquardt algorithms. The trained ANN model was extended to predict the real-field performance prediction of a full-scale CPV system of any size capacity, instead of just a single MJC. Due to the complex and non-linear behavior of MJCs, especially in the concentrated photovoltaic (CPV) configuration, the ANN-based approach has simplified the link between input and output parameters. Instead of going through time-extensive evaluations of thermal gradients for different irradiance concentration levels, the ANN model can simplify the prediction with the use of raw input values of the irradiance concentration and cell temperature. By knowing the solar potential and weather data of a certain location, the long-term field production of the CPV system can be easily predicted with the proposed ANN model.

Data availability statement

The original contributions presented in the study are included in the article/Supplementary Material; further inquiries can be directed to the corresponding authors.

Author contributions

MB wrote the manuscript. AS, MB, QC, and SO discussed and analyzed the results and reviewed the manuscript. SO provided the funding.

Funding

This work was supported by the Renewable Surplus Sector Coupling Technology Program of the Korean Institute of Energy Technology Evaluation and Planning (KETEP) and was granted financial resources from the Ministry of Trade, Industry, and Energy, Republic of Korea (No. 20226210100050).

Conflict of interest

The authors declare that the research was conducted in the absence of any commercial or financial relationships that could be construed as a potential conflict of interest.

Publisher's note

All claims expressed in this article are solely those of the authors and do not necessarily represent those of their affiliated organizations, or those of the publisher, the editors, and the reviewers. Any product that may be evaluated in this article, or claim that may be made by its manufacturer, is not guaranteed or endorsed by the publisher.

References

Almonacid, F., Fernandez, E. F., Mellit, A., and Kalogirou, S. (2017). Review of techniques based on artificial neural networks for the electrical characterization of concentrator photovoltaic technology. *Renew. Sustain. Energy Rev.* 75, 938–953. doi:10.1016/j.rser.2016.11.075

Almonacid, F., Fernández, E. F., Rodrigo, P., Pérez-Higueras, P. J., and Rus-Casas, C. (2013). Estimating the maximum power of a high concentrator photovoltaic (HCPV) module using an artificial neural network. *Energy* 53, 165–172. doi:10.1016/j.energy.2013.02.024

Almonacid, F., Rus, C., Pérez-Higueras, P., and Hontoria, L. (2011). Calculation of the energy provided by a PV generator. Comparative study: Conventional methods vs. artificial neural networks. *Energy* 36 (1), 375–384. doi:10.1016/j.energy.2010.10.028

Almonacid, F. J., Rus, C., Hontoria, L., and Munoz, F. J. (2010). Characterisation of PV CIS module by artificial neural networks. A comparative study with other methods. *Renew. Energy* 35 (5), 973–980. doi:10.1016/j.renene.2009.11.018

assets (2020). National renewable energy laboratory (NREL). Date retrieved https://www.nrel.gov/pv/assets/pdfs/best-research-cell-efficiencies.20200406.pdf 06 15, 2020).

Bailek, N., Bouchouicha, K., Aoun, N., Mohamed, E. S., Jamil, B., and Mostafaeipour, A. (2018). Optimized fixed tilt for incident solar energy maximization on flat surfaces located in the Algerian Big South. *Sustain. Energy Technol. Assessments* 28, 96–102. doi:10.1016/j.seta.2018.06.002

Bernal-Agustin, J. L., and Dufo-Lopez, R. (2009). Simulation and optimization of stand-alone hybrid renewable energy systems. *Renew. Sustain. Energy Rev.* 13, 2111–2118. doi:10.1016/j.rser.2009.01.010

Burhan, M., Chen, Q., Shahzad, M. W., Ybyraiymkul, D., Akhtar, F. H., and Ng, K. C. (2021). Innovative concentrated photovoltaic thermal (CPV/T) system with combined hydrogen and MgO based storage. *Int. J. Hydrogen Energy* 46, 16534–16545. doi:10.1016/j.ijhydene.2020.09.163

Burhan, M., Chua, K. J., and Ng, K. C. (2016). Long term hydrogen production potential of concentrated photovoltaic (CPV) system in tropical weather of Singapore. *Int. J. Hydrogen Energy* 41 (38), 16729–16742. doi:10.1016/j.ijhydene.2016.07.183

Burhan, M., Chua, K. J., and Ng, K. C. (2016). Simulation and development of a multi-leg homogeniser concentrating assembly for concentrated photovoltaic (CPV) system with electrical rating analysis. *Energy Convers. Manag.* 116, 58–71. doi:10.1016/j.enconman.2016.02.060

Burhan, M., Chua, K. J., and Ng, K. C. (2016). Sunlight to hydrogen conversion: Design optimization and energy management of concentrated photovoltaic (CPV-Hydrogen) system using micro genetic algorithm. *Energy* 99, 115–128. doi:10.1016/j.energy.2016.01.048

Burhan, M., Oh, S. J., Chua, K. J., and Ng, K. C. (2016). Double lens collimator solar feedback sensor and master slave configuration: Development of compact and low cost two axis solar tracking system for CPV applications. *Sol. Energy* 137, 352–363. doi:10.1016/j.solener.2016.08.035

Burhan, M., Oh, S. J., Chua, K. J., and Ng, K. C. (2017). Solar to hydrogen: Compact and cost effective CPV field for rooftop operation and hydrogen production. *Appl. energy* 194, 255–266. doi:10.1016/j.apenergy.2016.11.062

Burhan, M., Shahzad, M. W., and Ng, K. C. (2019). A universal theoretical framework in material characterization for tailored porous surface design. *Sci. Rep.* 9 (1), 8773–8777. doi:10.1038/s41598-019-45350-5

Burhan, M., Shahzad, M. W., and Ng, K. C. "Compact CPV—sustainable approach for efficient solar energy capture with hybrid concentrated photovoltaic thermal (CPVT) system and hydrogen production," in *The energy and sustainability 2018 symposium 2018* (Berlin/Heidelberg, Germany: Springer), 93–102.

Burhan, M., Shahzad, M. W., and Ng, K. C. (2019). "Concentrated photovoltaic (CPV) for rooftop—compact system approach," in *InAdvances in solar energy research* (Singapore: Springer), 157–174.

Burhan, M., Shahzad, M. W., and Ng, K. C. (2019). "Concentrated photovoltaic (CPV): From deserts to rooftops," in *InAdvances in sustainable energy* (Cham: Springer), 93–111.

Burhan, M., Shahzad, M. W., and Ng, K. C. (2018). "Concentrated photovoltaic (CPV): Hydrogen design methodology and optimization," in *InAdvances in hydrogen generation technologies* (London, UK: IntechOpen).

Burhan, M., Shahzad, M. W., and Ng, K. C. (2017). Development of performance model and optimization strategy for standalone operation of CPV-hydrogen system utilizing multi-junction solar cell. *Int. J. Hydrogen Energy* 42 (43), 26789–26803. doi:10.1016/j.ijhydene.2017.08.186

Burhan, M., Shahzad, M. W., and Ng, K. C. (2018). Energy distribution function based universal adsorption isotherm model for all types of isotherm. *Int. J. Low-Carbon Technol.* 13 (3), 292–297. doi:10.1093/ijlct/cty031

Burhan, M., Shahzad, M. W., and Ng, K. C. (2018). Hydrogen at the rooftop: Compact CPV-hydrogen system to convert sunlight to hydrogen. *Appl. Therm. Eng.* 132, 154–164. doi:10.1016/j.applthermaleng.2017.12.094

Burhan, M., Shahzad, M. W., and Ng, K. C. (2017). Long-term performance potential of concentrated photovoltaic (CPV) systems. *Energy Convers. Manag.* 148, 90–99. doi:10.1016/j.enconman.2017.05.072

Burhan, M., Shahzad, M. W., Oh, S. J., and Ng, K. C. (2018). A pathway for sustainable conversion of sunlight to hydrogen using proposed compact CPV system. *Energy Convers. Manag.* 165, 102–112. doi:10.1016/j.enconman.2018.03.027

Chen, Q., Oh, S. J., and Burhan, M. (2020). Design and optimization of a novel electrowetting-driven solar-indoor lighting system. *Appl. Energy* 269. doi:10.1016/j.apenergy.2020.115128115128

Cherucheril, G., March, S., and Verma, A. (2011). *Multijunction solar cells*. Coimbatore, India: Department of Electrical Engineering Iowa State University.

Cho, Y., Shaygan, A., and Daim, T. U. (2019). Energy technology adoption: Case of solar photovoltaic in the Pacific Northwest USA. *Sustain. Energy Technol. Assessments* 34, 187–199. doi:10.1016/j.seta.2019.05.011

Ghritlahre, H. K., Chandrakar, P., and Ahmad, A. (2020). Application of ANN model to predict the performance of solar air heater using relevant input parameters. *Sustain. Energy Technol. Assessments* 40. doi:10.1016/j.seta.2020.100764100764

Hakimi, S. M., Hajizadeh, A., Shafie-khah, M., and Catalão, J. P. (2020). Demand response and flexible management to improve microgrids energy efficiency with a high share of renewable resources. *Sustain. Energy Technol. Assessments* 42. doi:10.1016/j.seta.2020.100848100848

Homer (2015). Hybrid optimization of multiple energy resources. Available from: http://www.homerenergy.com/software.html.

iHOGA (2004). Improved hybrid optimization by genetic algorithms. Available from http://personal.unizar.es/rdufo/index.php?option=com_content&view=article&id=2&Itemid=104&lang=en.

Kalogirou, S. A. (2000). Applications of artificial neural-networks for energy systems. *Appl. energy* 67 (1-2), 17–35. doi:10.1016/s0306-2619(00)00005-2

Lampinen, J., and Vehtari, A. (2001). Bayesian approach for neural networks—Review and case studies. *Neural Netw.* 14 (3), 257–274. doi:10.1016/s0893-6080(00)00098-8

Mellit, A., Benghanem, M., Arab, A. H., and Guessoum, A. (2005). A simplified model for generating sequences of global solar radiation data for isolated sites: Using artificial neural network and a library of Markov transition matrices approach. *Sol. energy* 79 (5), 469–482. doi:10.1016/j.solener.2004.12.006

Mellit, A., Benghanem, M., Arab, A. H., and Guessoum, A. (2005). An adaptive artificial neural network model for sizing stand-alone photovoltaic systems: Application for isolated sites in Algeria. *Renew. energy* 30 (10), 1501–1524. doi:10.1016/j.renene.2004.11.012

Mellit, A., Benghanem, M., and Kalogirou, S. A. (2006). An adaptive wavelet-network model for forecasting daily total solar-radiation. *Appl. Energy* 83 (7), 705–722. doi:10.1016/j.apenergy.2005.06.003

Mellit, A., Benghanem, M., and Kalogirou, S. A. (2007). Modeling and simulation of a stand-alone photovoltaic system using an adaptive artificial neural network: Proposition for a new sizing procedure. *Renew. energy* 32 (2), 285–313. doi:10.1016/j.renene.2006.01.002

Motahar, S., and Bagheri-Esfeh, H. (2020). Artificial neural network based assessment of grid-connected photovoltaic thermal systems in heating dominated regions of Iran. *Sustain. Energy Technol. Assessments* 39. doi:10.1016/j.seta.2020.100694100694

Muhammad, B., Seung, J. O., Ng, K. C., and Chun, W. O. (2016). Experimental investigation of multijunction solar cell using two axis solar tracker. *InApplied Mech. Mater.* 818, 213–218. Trans Tech Publications Ltd. doi:10.4028/www.scientific.net/AMM.818.213

Nrel (2022). Best research-cell efficiency chart. Date retrieved https://www.nrel.gov/pv/cell-efficiency.html August 04, 2022).

Oh, S. J., Burhan, M., Ng, K. C., Kim, Y., and Chun, W. (2015). Development and performance analysis of a two-axis solar tracker for concentrated photovoltaics. *Int. J. Energy Res.* 39 (7), 965–976. doi:10.1002/er.3306

Peng, M. Y., Chen, C., Peng, X., and Marefati, M. (2020). Energy and exergy analysis of a new combined concentrating solar collector, solid oxide fuel cell, and steam turbine CCHP system. *Sustain. Energy Technol. Assessments* 39. doi:10.1016/j.seta.2020.100713100713

Rivera, A. J., García-Domingo, B., del Jesus, M. J., and Aguilera, J. (2013). Characterization of concentrating photovoltaic modules by cooperative competitive radial basis function networks. *Expert Syst. Appl.* 40 (5), 1599–1608. doi:10.1016/j.eswa.2012.09.016

Shahzad, M. W., Burhan, M., Ang, L., and Ng, K. C. (2017). Energy-water-environment nexus underpinning future desalination sustainability. *Desalination* 413, 52–64. doi:10.1016/j.desal.2017.03.009

Theristis, M., Fernández, E. F., Stark, C., and O'Donovan, T. S. (2016). A theoretical analysis of the impact of atmospheric parameters on the spectral, electrical and thermal performance of a concentrating III–V triple-junction solar cell. *Energy Convers. Manag.* 117, 218–227. doi:10.1016/j.enconman.2016.03.036

Zeynali, S., Rostami, N., Ahmadian, A., and Elkamel, A. (2020). Two-stage stochastic home energy management strategy considering electric vehicle and battery energy storage system: An ANN-based scenario generation methodology. *Sustain. Energy Technol. Assessments* 39. doi:10.1016/j.seta.2020.100722100722

10.3389/fenrg.2023.1067623

Nomenclature

$\mathbf{A_C}$ Solar cell area (m^2)

DNI Direct normal irradiance

$\mathbf{P_{MJC}}$ Power output of multi-junction solar cells (W)

$\mathbf{I_{mppt}}$ Solar cell maximum power point current (A)

$\boldsymbol{\eta}_{\mathbf{CPV}}$ Efficiency of the CPV module (%)

$\mathbf{P_{CPV}}$ CPV power output (W)

$\mathbf{P_{Input}}$ Solar energy input in the solar cell area (W)

$\mathbf{A_{lens}}$ Effective area of the solar concentrator (m^2)

$\mathbf{C_C}$ Solar concentration at the solar cell area (Sun)

$\mathbf{N_C}$ Number of solar cells in one panel

$\mathbf{V_{mppt}}$ Solar cell maximum power point voltage (V)

$\boldsymbol{\eta}_{\mathbf{OP}}$ Optical efficiency of the concentrating assembly (%)

$\boldsymbol{\eta}_{\mathbf{MJC}}$ Efficiency of MJCs (%)

$\mathbf{T_C}$ Solar cell temperature (°C)

10.3389/fenrg.2023.1067623

Appendix

TABLE A1 Experimental dataset.

T_c = 25°C		T_c = 35°C		T_c = 45°C		T_c = 60°C		T_c = 70°C		T_c = 80°C		T_c = 90°C	
C_C	η_{MJC}	C_C	η_{MJC}	C_C	η_{MJC}	C_C	η_{MJC}	C_C	η_{MJC}	C_C	η_{MJC}	C_C	η_{MJC}
10	36.3	15	35.5	16	34.8	10	33.4	18	32.3	10	31.4	10	30.8
15	36.5	25	35.9	20	35.0	20	33.7	28	32.7	15	31.6	20	31.2
19	36.6	35	36.2	25	35.1	30	34.1	61	33.9	19	31.8	30	31.6
26	36.9	59	36.8	32	35.4	40	34.4	75	34.2	26	32.1	40	32.0
30	37.0	75	37.2	42	35.7	67	35.2	87	34.5	30	32.2	67	32.8
33	37.1	81	37.3	56	36.1	86	35.6	105	34.9	33	32.3	86	33.3
39	37.2	100	37.7	64	36.3	96	35.8	110	35.0	39	32.5	96	33.5
47	37.4	111	37.9	76	36.5	110	36.0	119	35.2	59	33.2	110	33.8
55	37.6	120	38.0	86	36.7	123	36.2	130	35.3	75	33.6	123	34.0
60	37.7	138	38.2	95	36.9	135	36.4	140	35.5	81	33.8	145	34.3
77	38.1	159	38.4	104	37.1	150	36.5	155	35.6	100	34.2	162	34.4
86	38.2	170	38.5	110	37.2	155	36.6	175	35.8	111	34.4	175	34.6
95	38.4	180	38.6	130	37.5	163	36.7	193	35.9	120	34.5	180	34.6
100	38.5	195	38.6	145	37.6	175	36.8	200	36.0	138	34.8	195	34.7
112	38.6	205	38.7	162	37.8	185	36.8	210	36.0	159	35.0	218	34.8
119	38.7	215	38.7	175	37.9	190	36.9	215	36.1	170	35.1	225	34.8
134	38.9	220	38.7	180	38.0	200	36.9	225	36.1	180	35.2	240	34.9
145	39.0	229	38.8	195	38.1	205	36.9	240	36.2	195	35.3	255	34.9
160	39.1	237	38.8	218	38.2	210	37.0	250	36.2	218	35.4	260	34.9
164	39.1	250	38.8	225	38.2	220	37.0	260	36.2	225	35.4	270	35.0
179	39.2	254	38.8	240	38.3	230	37.0	275	36.2	240	35.5	279	35.0
200	39.3	265	38.9	255	38.3	240	37.1	295	36.3	255	35.5	299	35.0
209	39.4	273	38.9	260	38.3	253	37.1	310	36.3	260	35.5	310	35.0
215	39.4	285	38.9	270	38.4	288	37.2	324	36.3	270	35.6	324	35.0
231	39.4	290	38.9	279	38.4	305	37.2	340	36.3	279	35.6	340	35.0
240	39.4	300	38.9	299	38.4	325	37.2	350	36.3	299	35.6	350	35.0
271	39.5	315	38.9	310	38.4	350	37.2	361	36.3	310	35.6	361	35.0
288	39.5	330	38.9	319	38.4	360	37.2	369	36.3	319	35.6	369	35.1
295	39.5	335	38.9	325	38.4	378	37.3	373	36.4	325	35.6	373	35.1
305	39.5	343	38.9	335	38.4	385	37.3	386	36.4	350	35.6	386	35.1
316	39.5	360	38.9	350	38.4	394	37.3	392	36.4	360	35.6	392	35.1
330	39.5	367	38.9	355	38.4	410	37.3	400	36.4	378	35.6	400	35.1
345	39.5	375	38.9	361	38.4	424	37.3	415	36.4	385	35.6	415	35.1
350	39.5	382	38.9	369	38.4	431	37.3	430	36.4	394	35.6	430	35.1
368	39.5	395	38.9	387	38.4	447	37.3	445	36.4	410	35.6	445	35.1

(Continued on following page)

10.3389/fenrg.2023.1067623

TABLE A1 (*Continued*) Experimental dataset.

T_c = 25°C		T_c = 35°C		T_c = 45°C		T_c = 60°C		T_c = 70°C		T_c = 80°C		T_c = 90°C	
C_C	η_{MJC}	C_C	η_{MJC}	C_C	η_{MJC}	C_C	η_{MJC}	C_C	η_{MJC}	C_C	η_{MJC}	C_C	η_{MJC}
385	39.5	410	38.9	405	38.4	464	37.3	457	36.4	424	35.7	457	35.2
390	39.5	425	38.9	425	38.4	470	37.3	475	36.4	431	35.7	475	35.2
400	39.5	434	38.9	440	38.4	480	37.3	490	36.4	447	35.7	480	35.2
420	39.5	448	38.9	452	38.4	488	37.3	500	36.4	464	35.7	488	35.2
445	39.5	464	38.9	475	38.4	499	37.3	515	36.4	470	35.7	499	35.2
475	39.5	470	38.9	490	38.4	510	37.3	522	36.4	480	35.7	510	35.2
500	39.5	484	38.9	500	38.4	525	37.3	530	36.4	488	35.7	525	35.2
510	39.5	500	38.9	520	38.4	530	37.3	540	36.3	499	35.7	530	35.2
520	39.5	525	38.9	530	38.4	540	37.2	543	36.3	525	35.7	540	35.2
550	39.4	545	38.8	550	38.3	550	37.2	549	36.3	545	35.7	550	35.2